Springer Series in Computational Mathematics 47

Sören Bartels

Numerical Methods for Nonlinear Partial Differential Equations

Springer

Springer Series in Computational Mathematics

Volume 47

More information about this series at http://www.springer.com/series/797

Sören Bartels

Numerical Methods for Nonlinear Partial Differential Equations

Springer

Sören Bartels
Abteilung für Angewandte Mathematik
Albert-Ludwigs-Universität Freiburg
Freiburg
Germany

ISSN 0179-3632
Springer Series in Computational Mathematics
ISBN 978-3-319-13796-4 ISBN 978-3-319-13797-1 (eBook)
DOI 10.1007/978-3-319-13797-1

Library of Congress Control Number: 2014957868

Mathematics Subject Classification (2010): 65N30, 65N12, 65M12, 65M22, 65K15, 49M15, 49M29

Springer Cham Heidelberg New York Dordrecht London

Printed on acid-free paper

Springer International Publishing AG Switzerland is part of Springer Science+Business Media (www.springer.com)

Contents

Chapter 1
Introduction

As Henri Poincaré once remarked, "solution of a mathematical problem" is a phrase of indefinite meaning. Pure mathematicians sometimes are satisfied with showing that the nonexistence of a solution implies a logical contradiction, while engineers might consider a numerical result as the only reasonable goal. Such one-sided views seem to reflect human limitations rather than objective values.

– Richard Courant, 1941

1.1 Differential Equations and Numerical Methods

Starting with the brachistochrone problem solved by Johann Bernoulli in the 17th century, differential equations have become an indispensable tool to model, understand, and solve real world problems. The general approach via the Euler–Lagrange equations related to a variational principle and Euler's method to approximately solve differential equations discovered in the 18th century have provided a methodology that is still the basis for the mathematical modeling and numerical solution of many problems describing the behavior of solids and fluids. An important part of those models is the Laplace equation which is the Euler–Lagrange equation for the Dirichlet energy. The validity of the Dirichlet principle that postulates the existence of minimizers and hence solutions of Euler–Lagrange equations led to a controversial but constructive discussion in the 19th century. Important observations and objections from Cauchy, Riemann, Weierstraß, Schwarz, Ritz, and many others resulted in the birth of the calculus of variations and the finite element method. These mathematical concepts were led to concise mathematical theories by Hilbert and Courant at the beginning of the 20th century.

The abstract investigation of function spaces with topologies, functionals, and linear operators in the 20th century associated with deep theorems due to Banach and others, led to formulating the direct method in the calculus of variations in an

S. Bartels, *Numerical Methods for Nonlinear Partial Differential Equations*,
Springer Series in Computational Mathematics 47,
DOI 10.1007/978-3-319-13797-1_1

abstract way. This enabled the study of challenging mathematical problems involving the efficient description of processes on nanoscales and to establishing rigorous connections between classical models like three-dimensional elasticity and special applications involving the deformation of lower-dimensional objects. The development of functional analysis also had an impact in understanding numerical methods. A milestone is the construction of compatible finite element spaces and the rigorous analysis of problems involving linear constraints or higher-order derivatives within the inf-sup condition as an application of the closed range theorem.

The development of mixed and adaptive finite element methods, multigrid and domain decomposition algorithms, as well as wavelet and other compression techniques, in combination with the rapidly increasing available computer power in the last 50 years, have made it possible to compute forces acting on a bridge, turbulences created by the flow of air around an airplane, or compression of digital objects within minutes or seconds on personal computers. In parallel, the calculus of variations has become a powerful mathematical discipline that provides a framework for the effective description of complicated phenomena, such as microstructures in crystalline solids or the formation of cracks in materials with abstract mathematical objects such as measures. The price of these impressive individual advances of initially closely linked disciplines has led to a separation from them. Many powerful numerical techniques are difficult to analyze, while a lot of abstract analytical concepts are hard to realize practically. This book aims at contributing towards closing this gap.

1.2 Guidelines for the Development of Approximation Schemes

The classical numerical analysis of approximation schemes for partial differential equations exploits the concepts of stability and regularity. These are strong requirements that are available for certain classes of linear elliptic and parabolic equations. In many modern applications, solutions may be neither unique nor regular, and stability has to be formulated in a weaker sense. Possible concepts are weak convergence methods and convergence of minimizers. These approaches avoid making unrealistic regularity or uniqueness assumptions but justify rigorous approximation schemes. Since this leads to asymptotic statements, the efficiency and practical accuracy of these schemes then needs to be studied separately. We formulate some guidelines to justify a numerical discretization scheme.

The discretization of a variational problem or partial differential equation called a continuous problem typically leads to a family of finite-dimensional minimization problems:

$$\text{Minimize } I_h(u_h) \text{ in the set of functions } u_h \in \mathscr{A}_h$$

or equations

$$\text{Find } u_h \in \mathscr{A}_h \text{ such that } F_h(u_h) = 0$$

parametrized by a mesh-size $h > 0$. The main tasks in the development and justification of discretizations are the following:
(a) *Qualitative accuracy*: A numerical solution u_h should capture the relevant features of an exact solution u with a small number of degrees of freedom, e.g., if ε is a characteristic length scale of the problem under consideration, then the numerical method should provide qualitatively correct solutions with a computational length scale $h \approx \varepsilon/10$.
(b) *Efficient solution*: There should exist an iterative and convergent method that approximately solves the discrete formulation with a computational effort that scales like a low-order polynomial in the number of degrees of freedom, e.g., a fixed-point method or a gradient flow converges within a finite number of iterations and provides an approximation of a discrete solution with a solution error comparable to a power of h.
(c) *Asymptotic convergence*: A relevant quantity related to approximate solutions should converge to a corresponding quantity for the continuous problem as $h \to 0$, e.g., the approximate minimal energies $I_h(u_h)$ converge to $\inf_{u \in \mathscr{A}} I(u)$, subsequences of approximations converge to solutions of the continuous problem, or certain quantities $\sigma_h = \Sigma_h(u_h)$ converge to a meaningful quantity σ as $h \to 0$.

We investigate these requirements for certain prototypical nonlinear partial differential equations arising in the mathematical modeling of contact, phase transitions, ferromagnetism, bending, microstructures, fracture, and plasticity. The related model problems have in common that the regularity or uniqueness of solutions fails in general, so that numerical schemes have to be carefully developed in order to meet the aforementioned criteria. Short MATLAB implementations are included for most of the investigated algorithms that allow for testing the dependence of the performance on discretization parameters and for experimentally determining the typical preasymptotic range of the methods to thereby judge their qualitative accuracy.

1.3 Analytical and Numerical Foundations

The contents of this monograph are divided into three parts. The first provides the analytical framework for the considered model problems, collects the basic results related to the finite element method, and formulates abstract concepts for the analysis and solution of discretized problems. In the second part, the numerical solution of classical nonlinear partial differential equations, such as problems with inequality constraints, singularly perturbed parabolic equations, variational formulations with smooth constraints, and problems involving higher-order derivatives are discussed. In the third part, the approximation of solutions of nonstandard variational models is discussed on the basis of nonconvex minimization problems, extended formulations

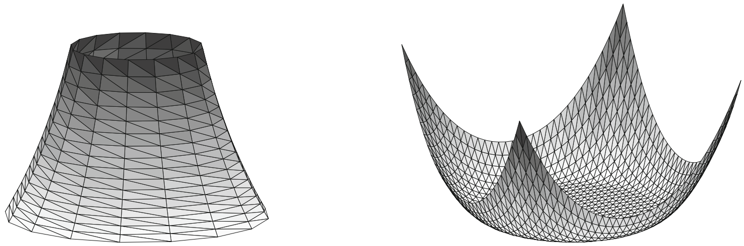

Fig. 1.1 Discrete minimal surface computed with a descent method (*left*) and solution of an obstacle problem computed with a semismooth Newton iteration (*right*); the plots were produced with the MATLAB routines `min_surf.m` and `obstacle_newton.m`

allowing for solutions with strong discontinuities, and nonsmooth, rate-independent evolution problems.

The mathematical model problems studied in this book are introduced and briefly described in the first chapter. All of them lead to minimization problems defined in certain function spaces or to evolution problems that are gradient flows of functionals. The basic techniques to study the existence and uniqueness of solutions can be addressed in the direct method in the calculus of variations and the concept of gradient or subdifferential flows that are described in Chap. 2. Chapter 3 introduces the finite element method and its analysis for linear elliptic and parabolic problems. Various auxiliary estimates such as inverse inequalities and density results as well as error estimates in different norms are recalled. In Chap. 4 general abstract methods for analyzing discretized problems and their iterative solutions are formulated. Key concepts are the variational convergence of discrete minimization problems to a corresponding continuous one, and the convergence of discretized partial differential equations. The different performance of iterative solution methods is illustrated by computing discrete minimal surfaces with large, unbounded gradients, as shown in the left plot of Fig. 1.1.

1.4 Approximation of Classical Formulations

The obstacle problem is a classical mathematical model problem that serves to understand inequality constraints in partial differential equations. The existence and uniqueness of solutions, the justification of numerical schemes with a priori and a posteriori error estimates, and the iterative solution with semismooth Newton methods are discussed in Chap. 5. The right plot of Fig. 1.1 shows the numerical solution of a two-dimensional obstacle problem with circular contact zone.

The evolution of an interface separating two phases of a substance is often based on the introduction of a phase field variable. The corresponding dynamics are modeled by the gradient flow of an energy functional with nonconvex lower-order terms leading to semilinear parabolic partial differential equations involving a critical para-

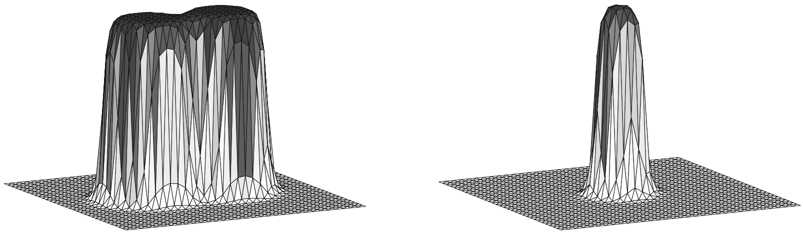

Fig. 1.2 Snapshots of a phase field variable in an Allen–Cahn evolution computed with a semi-implicit approximation scheme; the numerical solution was obtained with the MATLAB program `ac_linearized_euler.m`

meter that determines the width of the interfaces. Standard discretization methods provide useful approximations but error estimates typically depend exponentially on the inverse of the critical parameter. Chapter 6 provides an approach that leads to robust error estimates. When the critical parameter tends to zero, a so-called sharp interface model can be identified that determines the evolution of the interface in terms of its geometric properties. Figure 1.2 shows snapshots of an evolution for different times. The initial interface deforms into a sphere whose radius decreases gradually and eventually collapses. This is a simplified model for the description of certain melting processes.

The character of a problem changes significantly when a pointwise equality constraint is imposed, e.g., when a vector field attains its values in the zero level set of a given function. This leads to the notion of harmonic maps which are discussed in Chap. 7. Since neither uniqueness nor global regularity results are available, only the accumulation of approximations with respect to a weak topology at exact solutions can be shown. The pointwise constraint is imposed at the nodes of a triangulation and various iterative methods that either preserve the constraint via properties of the underlying partial differential equation or approximate it by a linearization and a subsequent optional projection are discussed. Figure 1.3 displays views of a harmonic map from a two-dimensional square into the two-dimensional unit sphere.

A dimension reduction from three-dimensional hyperelasticity in the bending regime leads to the nonlinear Kirchhoff model for the description of large deforma-

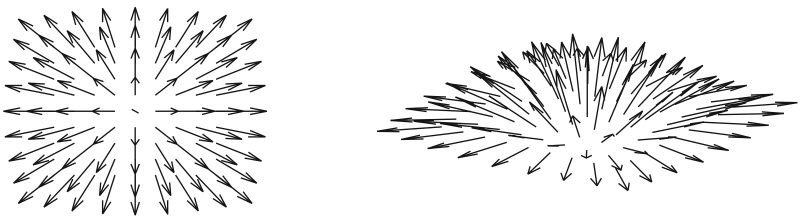

Fig. 1.3 Discrete harmonic map into the unit sphere viewed from two different perspectives; the iterative scheme realized in the MATLAB program `h1_flow_hm.m` led to the plots

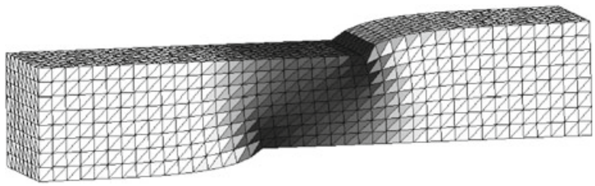

Fig. 1.4 Concentration of plastic strains in an elastoplastic compression experiment with small hardening parameter; the numerical solution of the nonlinear, nonsmooth evolution problem was computed with the MATLAB routine `elastoplasticity.m`

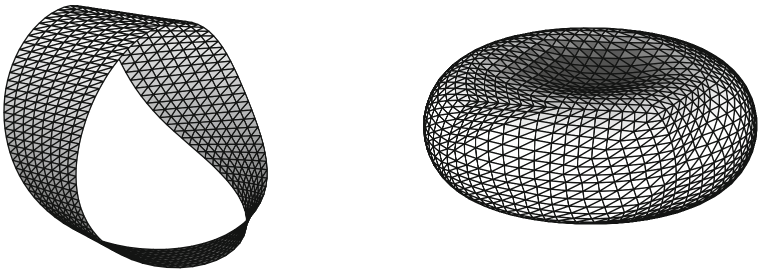

Fig. 1.5 Isometric deformation of a flat rectangular strip (*left*) and stationary configuration of the bending energy among closed surfaces with prescribed area and enclosed volume (*right*); the solutions were computed with the MATLAB routines `kirchhoff_nonlinear.m` and `willmore_helfrich_flow.m`

tions of two-dimensional objects, e.g., the bending of a sheet of paper. In the reduced model, local angle and area relations are preserved by the deformation and this is mathematically described by a pointwise isometry constraint which can be treated with techniques developed for harmonic maps. The additional numerical difficulty that higher-order derivatives have to be treated can be solved by employing finite element methods that were originally developed for linear bending problems describing small displacements. The resulting numerical scheme is provided in Chap. 8 and can be employed to compute the Möbius strip as the deformation of a flat strip of minimal bending energy subject to Dirichlet type boundary conditions at the ends of the strip. The result of a simulation with only a few degrees of freedom is shown in Fig. 1.5. A closely related problem consists in minimizing the Willmore energy in closed surfaces of a prescribed surface area and enclosed volume. Starting a gradient flow with an oblate spheroid, the gradient flow becomes stationary at a discocyte configuration that resembles the shape of a red blood cell. A low-order finite element scheme produced the plot shown in Fig. 1.5.

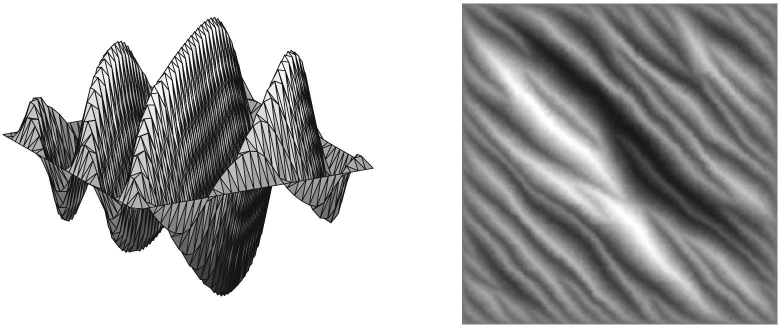

Fig. 1.6 Direct numerical minimization of a nonconvex energy functional leading to mesh-dependent oscillations on a coarse (*left*) and on a fine grid (*right*); the steepest descent method that computed the local minimizers is realized in the MATLAB program `energy_minimization.m`

1.5 Numerical Methods for Extended Formulations

The third part of the monograph investigates problems that are in general ill-posed within the classical framework of Sobolev spaces, e.g., provided by the direct method in the calculus of variations when an energy functional is coercive and weakly lower semicontinuous, and the underlying space is reflexive. Simple mathematical models for crystalline phase transitions lead to nonconvex energy densities which violate the semicontinuity requirement. Infimizing sequences still exist, but their accumulation points are in general no minimizers. This phenomenon is related to the occurrence of oscillations in the infimizing sequences that compensate for the nonconvexity of the energy functional. The weak limits and statistical information about the oscillations, described by Young measures, are relevant quantities in applications and their numerical approximation is discussed in Chap. 9. Figure 1.6 shows the results of a direct numerical approach based on minimizing the nonconvex energy functional with a descent method. The numerical approximations develop oscillations whose frequencies increase when the mesh is refined. The obtained configurations cannot be expected to be global minimizers, making their practical relevance unclear. Therefore, other approaches are required to obtain meaningful information.

Another reason for the failure of the direct method in the calculus of variations is the nonreflexivity of the employed space. Applications in image processing and and fracture mechanics motivate considering energy densities with linear growth and extended function spaces need to be considered that allow for minimizers with strong discontinuities. The appropriate discretization, error estimates, and iterative solution methods for certain model problems are studied in Chap. 10. Figure 1.7 shows as an application the denoising of an image obtained by minimizing an energy that preserves the edges of the noisy image.

The focus of Chap. 11 is on nonsmooth evolution problems occurring in the mathematical modeling of elastoplastic material behavior. Viscous regularizations of evolution problems are of limited practical use in applications. Instead, approxi-

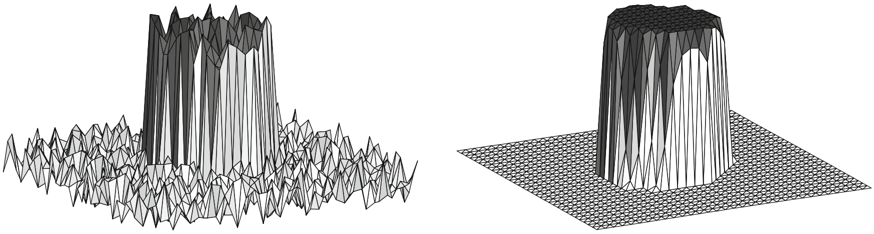

Fig. 1.7 Regularization of a noisy image (*left*) that preserves the edges of the image that are related to large, maximal gradients in the numerical approximation (*right*); the configurations were obtained with an iterative scheme realized in the MATLAB code `tv_reg.m`

mation schemes have to be developed which preserve the relevant property of rate-independence. Error estimates for implicit discretizations of the evolution problem in the case of kinematic and isotropic hardening are analyzed and their practical realization is discussed. The result of a numerical simulation based on the provided MATLAB codes displayed in Fig. 1.4 shows the tendency towards the development of a slip band in a compression experiment with small hardening parameter.

1.6 Objectives and Acknowledgments

The purpose of this work is to enable advanced students and experienced researchers to gain an entry into the numerical analysis of problems related to modern applications in continuum mechanics. Every chapter in the second and third part of the book starts with a review of the analytical properties of the model problem under consideration and gives selected references to provide links to detailed explanations and proofs. The main emphasis is on the development and analysis of approximation schemes that meet the general criteria outlined above. MATLAB implementations of the schemes that allow for a treatment of two- and three-dimensional problems are typically discussed at the end of the chapters. The codes are available at http://extras.springer.com/2015/978-3-319-13796-4. These implementations are meant to illustrate the simplicity and efficiency of the proposed schemes and to serve as reference codes that are easily accessible. Only a selected number of references is listed at the end of every chapter that serve as entries into the large number of relevant contributions.

The presented material is the result of several years of research, inspiration from numerous researchers' work, and discussions with many colleagues. I am grateful to Max Jensen, Martin Kružík, Marijo Milicevic, Rüdiger Müller, Ricardo H. Nochetto, Christoph Ortner, Alexis Papathanassopoulos, Andreas Prohl, Tomaš Roubíček, Patrick Schreier, Ulisse Stefanelli, and Mirjam Walloth for reading parts of the manuscript and giving me useful hints and comments.

Sören Bartels
Freiburg, September 2013

Part I
Analytical and Numerical Foundations

Chapter 2
Analytical Background

2.1 Variational Model Problems

We describe in this section some model problems that arise in the mathematical description of certain phenomena in continuum mechanics. For justifications of the models, the reader is referred to the textbooks [3, 5, 9, 11].

2.1.1 Deflection of a Membrane

We consider a membrane that occupies the domain $\Omega \subset \mathbb{R}^2$ and is clamped on its boundary $\partial\Omega$. The infinitesimal deflection due to a small vertical force $f \in L^2(\Omega)$ is described by the problem of minimizing the energy functional

$$I(u) = \frac{1}{2}\int_\Omega |\nabla u|^2 \,\mathrm{d}x - \int_\Omega f u \,\mathrm{d}x$$

in the set of functions $u \in H^1(\Omega)$ with $u|_{\partial\Omega} = 0$, cf. Fig. 2.1. The first term in the energy functional I is the *Dirichlet energy*. The Lax–Milgram lemma guarantees the existence of a unique solution that solves the corresponding *Euler–Lagrange equations* which are given by the *Poisson problem* $-\Delta u = f$ in Ω and $u|_{\partial\Omega} = 0$.

2.1.2 Minimal Surfaces

A mathematical model for describing soap films follows from the hypothesis that these minimize surface area. If the surface can be represented as the graph of a function $u : \Omega \to \mathbb{R}$, this leads to the variational problem of minimizing the functional

S. Bartels, *Numerical Methods for Nonlinear Partial Differential Equations*,
Springer Series in Computational Mathematics 47,
DOI 10.1007/978-3-319-13797-1_2

Fig. 2.1 Deflection of a membrane

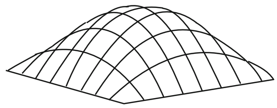

Fig. 2.2 Minimal surface described by a graph

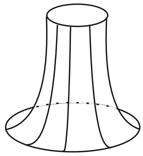

$$I(u) = \int_{\Omega} (1 + |\nabla u|^2)^{1/2} \, \mathrm{d}x$$

in the set of functions $u \in W^{1,p}(\Omega)$ for some appropriate exponent $p \in [1, \infty]$, subject to the boundary condition $u|_{\partial\Omega} = u_{\mathrm{D}}$. If one expects that $|\nabla u| \ll 1$, then the approximation $(1 + |\nabla u(x)|^2)^{1/2} \approx 1 + (1/2)|\nabla u|^2$ justifies using the Dirichlet energy and $p = 2$ to compute solutions. In the general case, the right choice of p is unclear and this is related to the limitations of the model which only applies to situations in which the entire surface is described by a graph. In general this is not true, and large unbounded gradients can occur in minimizing the energy related to functions that do not belong to $W^{1,p}(\Omega)$, cf. Fig. 2.2.

2.1.3 Hyperelastic Materials

Many solid materials behave in an elastic way for a large range of forces, i.e., when a force acts on the body it deforms and when the force stops acting, the body returns to its reference configuration, e.g., the material behaves like a sponge or a network of elastic springs, cf. Fig. 2.3. One can then justify that the actual *deformation* $y : \Omega \to \mathbb{R}^3$ of the body $\Omega \subset \mathbb{R}^3$, due to a force $f : \Omega \to \mathbb{R}^3$, such as gravity minimizes an energy functional of the form

$$I(y) = \int_{\Omega} W(\nabla y) \, \mathrm{d}x - \int_{\Omega} f \cdot y \, \mathrm{d}x$$

Fig. 2.3 Hyperelastic deformation of a beam

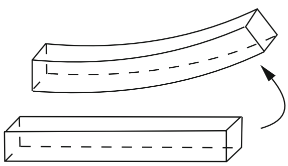

in the set of functions $y \in W^{1,p}(\Omega; \mathbb{R}^3)$ that satisfy boundary conditions $y|_{\Gamma_D} = y_D$ on a subset $\Gamma_D \subset \partial\Omega$. Various physical requirements limit possible choices of W, e.g., since a body cannot be compressed arbitrarily, we require that $W(F) \to \infty$ as $\det F \to 0$ with $\det F > 0$. Moreover, in the absence of a force, and for boundary conditions defined by a rotation of the body, the rotation should also minimize the energy, i.e., $DW(R) = 0$ for every $R \in SO(3)$. These two conditions imply that W cannot be convex. If the body is only slightly displaced from its reference configuration, i.e., $y = \mathrm{id} + u$ with the *displacement* $u : \Omega \to \mathbb{R}^3$ satisfying $|\nabla u| \ll 1$, then with $DW(I) = 0$ we have the approximation

$$W(\nabla[\mathrm{id} + u]) \approx W(I) + \frac{1}{2} D^2 W(I)[\nabla u, \nabla u]$$

which justifies replacing $W(\nabla y)$ by the quadratic expression $(1/2)\mathbb{C}\nabla u : \nabla u$ with the *elasticity tensor* $\mathbb{C} = D^2 W(I)$ and with $A : B$ denoting the inner product of two matrices. The resulting model of *linear elasticity* is important in many applications where only small strains occur.

2.1.4 Obstacle Problems

When the deflection of an elastic membrane is restricted by an *obstacle*, then a constraint has to be included in the above minimization problem, i.e., we seek $u \in H^1(\Omega)$ with $u|_{\partial\Omega} = u_D$, which is a solution of the constrained minimization problem defined by

$$I(u) = \frac{1}{2} \int_\Omega |\nabla u|^2 \, \mathrm{d}x - \int_\Omega f u \, \mathrm{d}x \quad \text{subject to } u \geq \chi \text{ in } \Omega.$$

It is not known in advance and depends on the force and the boundary conditions where the membrane will touch the obstacle described by the function χ. Therefore, determining a *free boundary* that separates the *contact zone* $\mathscr{C} = \{x \in \Omega : u(x) = \chi(x)\}$ from the *noncontact zone* is part of the problem. A model situation is illustrated in Fig. 2.4.

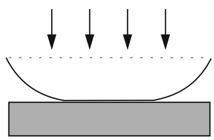

Fig. 2.4 Cross-section of the constrained deflection of a membrane

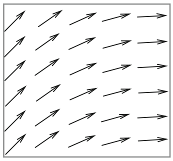

Fig. 2.5 Unit length vector field that may describe the orientation of liquid crystal molecules

2.1.5 Harmonic Maps

A different type of constraint arises in modeling certain liquid crystals and ferromagnets. If the vector field $u : \Omega \to \mathbb{R}^3$ describes the orientation of the rod-like molecules of a liquid crystal or the magnetization of a ferromagnet, then it is natural to impose the pointwise constraint $|u(x)| = 1$ in Ω. In a greatly simplified setting, we then consider the energy functional

$$I(u) = \frac{1}{2}\int_{\Omega} |\nabla u|^2 \,\mathrm{d}x \quad \text{subject to } |u(x)| = 1 \text{ in } \Omega,$$

together with boundary conditions such as $u|_{\Gamma_\mathrm{D}} = u_\mathrm{D}$. Solutions of this minimization problem are called *harmonic maps into the sphere*. Such vector fields can have strong singularities; a smooth unit-length vector field is depicted in Fig. 2.5.

2.1.6 Phase-Field Models

Pointwise constraints in minimization problems are often included by adding a *penalty term* to the energy functional, e.g., by considering

$$I(u) = \frac{1}{2}\int_{\Omega} |\nabla u|^2 \,\mathrm{d}x + \frac{1}{4\varepsilon^2}\int_{\Omega} (|u|^2 - 1)^2 \,\mathrm{d}x$$

with a small parameter $0 < \varepsilon \ll 1$. Deviations of the function $u : \Omega \to \mathbb{R}$ or the vector field $u : \Omega \to \mathbb{R}^3$ from unit length are thus strongly penalized, but in general minimizers will not satisfy $|u| = 1$ everywhere. In the case of a scalar function $u : \Omega \to \mathbb{R}$, this leads to the formation of an *interface* $\Gamma \subset \Omega$ that separates regions in which $u \approx 1$ and $u \approx -1$, cf. Fig. 2.6. The energy functional I with fixed ε occurs in modeling certain *phase transition models* and then the function u describes two different phases, such as a solid and a liquid phase by the values ± 1 and the interface via $\Gamma = \{x \in \Omega : u(x) = 0\}$.

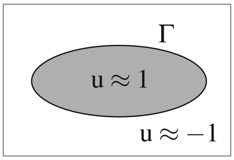

Fig. 2.6 A function that represents the phases in a binary phase separation process

2.1.7 Plate Bending

When the thickness of a hyperelastic body Ω is small, e.g., if $\Omega = \omega \times (-t/2, t/2)$ with a plate thickness $0 < t \ll 1$, then the behavior of the body changes drastically. In such situations it is desirable to treat the body as a two-dimensional object, i.e., to consider an appropriate limit $t \to 0$, described by the deformation of the mid-surface $\omega \subset \mathbb{R}^2$. For a large class of forces f and boundary conditions y_D, the minimal value of the three-dimensional energy minimization problem is proportional to t^3 called the bending regime, from which one then can rigorously derive a dimensionally reduced model that describes the deformation $y : \omega \to \mathbb{R}^3$ of the mid-surface ω via the constrained energy functional

$$I^{2D}(y) = \frac{1}{2}\int_\omega |D^2 y|^2 \,\mathrm{d}x - \int_\omega \tilde{f} \cdot y \,\mathrm{d}x \quad \text{subject to } \nabla y^\top \nabla y = I \text{ in } \Omega$$

together with the boundary conditions $y|_{\Gamma_D} = y_D$ and $\nabla y|_{\Gamma_D} = B_D$. The pointwise constraint on the deformation gradient implies that y is an *isometry*, i.e., that locally, length and angle relations are preserved. The model describes the deformation of a sheet of paper or a piece of cloth, cf. Fig. 2.7.

2.1.8 Crystalline Phase Transitions

For certain crystalline solids the structure of the crystal lattice is temperature-dependent and this enables many important technical applications based on the *shape-memory effect*. The underlying mechanism is that the crystal lattice is highly symmetric, e.g., cubic, for temperatures above a *transition temperature* θ_0 and less structured for low temperatures, e.g., tetragonal, cf. Fig. 2.8. In the low-temperature phase the material can be deformed easily, and in the high-temperature phase it is stiff

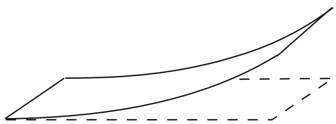

Fig. 2.7 Isometric deformation of a thin elastic sheet

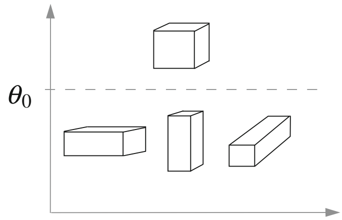

Fig. 2.8 Crystalline phase transition

and tends to return to its reference configuration. If the less structured crystal lattice is described by matrices $F_1, \ldots, F_J \in \mathbb{R}^{3\times 3}$, then a simplified model for the elastic deformation of the material below the transition temperature leads to minimizing the energy functional

$$I(y) = \int_\Omega W(\nabla y)\,\mathrm{d}x \quad \text{with} \quad W(F) = \min_{j=1,\ldots,J} \frac{1}{2}|F - F_j|^2.$$

The *nonconvexity* of the energy density W results in developing oscillations of the deformation gradient ∇y between the values $F_1, \ldots, F_J$. Due to the lack of a characteristic length scale, the oscillations become arbitrarily rapid and a minimizer of I may not exist. This fact requires that the model be appropriately modified in order to capture relevant information about the macroscopic material behavior.

2.1.9 Free-Discontinuity Problems

Many modern applications, including image processing and damage or fracture of materials, require describing certain quantities by discontinuous functions. One approach to their mathematical modeling is to consider a generalized, measure-valued gradient, and this allows us to treat functions that are piecewise smooth with an appropriate discontinuity set, e.g., the characteristic function of a square or a disk. In order to regularize a given noisy image described by its gray values by a function $g : \Omega \to \mathbb{R}$ while preserving its edges, the *total-variation regularized* model seeks a function $u : \Omega \to \mathbb{R}$ that minimizes the functional

$$I(u) = \int_\Omega |Du| + \frac{\alpha}{2}\|u - g\|^2_{L^2(\Omega)}.$$

The second term in the energy functional makes sure that u is close to g, while the first term prohibits certain oscillations, cf. Fig. 2.9. For weakly differentiable functions $u \in W^{1,1}(\Omega)$, the first term coincides with $\|\nabla u\|_{L^1(\Omega)}$, but it is also finite for a large class of discontinuous functions, e.g., if $u = \chi_A$ is the characteristic function of a set $A \subset \Omega$, then $\int_\Omega |Du|$ is the length of ∂A.

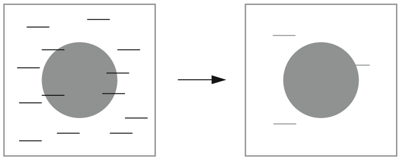

Fig. 2.9 Denoising of a perturbed image

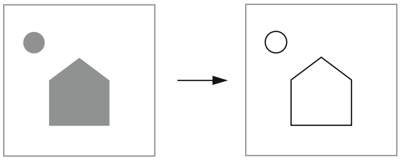

Fig. 2.10 Segmentation of an image

2.1.10 Segmentation Models

Modeling a crack in a material typically requires an explicit description of the crack. Similarly, the problem of detecting certain shapes in images can be described by considering the unknown contour of objects as a separate variable in a model. A simple model problem is defined by the *Mumford–Shah functional*

$$I(u, K) = \frac{1}{2} \int_{\Omega \setminus K} |\nabla u|^2 \, dx + \mathscr{H}^{d-1}(K) + \frac{\alpha}{2} \|u - g\|^2_{L^2(\Omega)}.$$

Here, $K \subset \overline{\Omega}$ is a closed subset and its $(d-1)$-dimensional Hausdorff measure $\mathscr{H}^{d-1}(K)$ is finite if K belongs to a class of certain lower-dimensional objects such as unions of curves for $d = 2$. A minimizing function $u \in L^2(\Omega)$ has to be weakly differentiable in $\Omega \setminus K$ and close to g, but it may jump and have discontinuities across K. The minimization problem detects contours in a given image g and identifies objects as depicted in Fig. 2.10.

2.1.11 Elastoplasticity

The restoring force or *stress* σ of an elastic spring or rubber band of initial length ℓ that is elongated by an external loading with *strain* $\varepsilon(u) = u'$ is according to *Hooke's law* given by $\sigma = \mathbb{C}\varepsilon(u)$ for a certain range of strains. When σ reaches a critical value σ_y called *yield stress*, then the material behavior changes and a remaining, *plastic* deformation occurs, i.e., after the experiment we observe that the length $\widetilde{\ell}$ of the rubber band is bigger than its initial length ℓ. This is accompanied by a change of the microstructural properties of the material, e.g., of the crystal lattice. Mathematically, this can be described by the requirement that $\sigma \in S = \overline{B_{\sigma_y}(0)}$ and that plastic material behavior occurs if $\sigma \in \partial S$. In this case an increasing strain

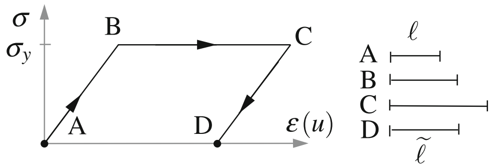

Fig. 2.11 Stress-strain relation for perfectly plastic material behavior; from A to B the material behaves elastically, from B to C a plastic strain occurs leading to a remaining deformation, and from C to D the elastic part of the deformation relaxes

$\varepsilon(u)$ is compensated by a developing *plastic strain* p, i.e., $\sigma = \mathbb{C}(\varepsilon(u) - p)$. The nonlinear stress-strain relation is depicted in Fig. 2.11. With the equilibrium of forces in a quasistatic situation, the process is modeled by the equations

$$-\operatorname{div}\sigma = f, \quad \varepsilon(u) = \mathbb{C}^{-1}\sigma + p, \quad \dot{p} \in \partial I_S(\sigma)$$

with ∂I_S denoting the subdifferential of the indicator functional of S which is the normal cone mapping related to the convex set S, i.e.,

$$\partial I_S(\sigma) = \begin{cases} \{0\} & \text{if } |\sigma| < \sigma_y, \\ \{\alpha\sigma : \alpha \geq 0\} & \text{if } |\sigma| = \sigma_y, \\ \emptyset & \text{if } |\sigma| > \sigma_y. \end{cases}$$

This is a time-dependent formulation and after discretization in time, one is led to solve for every time-step t_k the minimization problem

$$I^k(u, p) = \frac{\sigma_y}{\tau}\int_\Omega |p - p^{k-1}|\,\mathrm{d}x + \frac{1}{2}\int_\Omega |\mathbb{C}^{1/2}(\varepsilon(u) - p)|^2\,\mathrm{d}x - \int_\Omega f \cdot u\,\mathrm{d}x,$$

where p^{k-1} is the solution of the previous time step and subject to time-dependent boundary conditions $u|_{\Gamma_\mathrm{D}} = u_\mathrm{D}(t_k)$. In a more realistic description, deformations that are pure compressions or tensions do not lead to plastic deformations and only $|\operatorname{dev}(\sigma)| \leq \sigma_y$ is required with the *deviator* $\operatorname{dev} A = A - (1/d)(\operatorname{tr} A)I$ of a matrix $A \in \mathbb{R}^{d\times d}$. Moreover, additional variables are included to describe the internal properties of the material.

2.2 Existence of Minimizers

We discuss in this section sufficient and necessary conditions for the existence of minimizers for energy functionals of the form

$$I(u) = \int_{\Omega} W(x, u(x), \nabla u(x))\,\mathrm{d}x$$

in a set of weakly differentiable admissible functions $\mathscr{A} \subset W^{1,p}(\Omega;\mathbb{R}^m)$ for a bounded Lipschitz-domain $\Omega \subset \mathbb{R}^d$. The main idea is to develop an appropriate generalization of the Bolzano–Weierstraß theorem to infinite-dimensional situations. In particular, to deduce compactness properties of bounded sets, it is necessary to work with weak topologies and the usual continuity assumption is replaced by (weak) lower semicontinuity. For further details and more general statements the reader is referred to the textbooks [1, 4, 6, 10].

2.2.1 *The Direct Method in the Calculus of Variations*

We consider a functional $F : X \to \mathbb{R} \cup \{+\infty\}$ defined on a real, reflexive Banach space X and discuss the existence of minimizers of F.

Definition 2.1 The function $F : X \to \mathbb{R} \cup \{+\infty\}$ is called *weakly lower semicontinuous* if for every sequence $(v_n)_{n\in\mathbb{N}} \subset X$ and $v \in X$ with $v_n \rightharpoonup v$ as $n \to \infty$, i.e., $\phi(v_n) \to \phi(v)$ for every $\phi \in X'$, we have

$$F(v) \le \liminf_{n\to\infty} F(v_n).$$

The validity and the failure of the requirement are illustrated in Fig. 2.12.

Remarks 2.1 (i) The sequence $(F(v_n))_{n\in\mathbb{N}} \subset \mathbb{R} \cup \{+\infty\}$ may be divergent and the definition requires that $F(v)$ be a lower bound for all accumulation points of the sequence.
(ii) In infinite-dimensional spaces, weak lower semicontinuity is a stronger requirement than (strong) lower semicontinuity, i.e., $F(v) \le \liminf_{n\to\infty} F(v_n)$ whenever v_n converges (strongly) to v. Mazur's lemma implies that every convex, (strongly) lower semicontinuous functional is weakly lower semicontinuous. In finite-dimensional spaces the notions of weak and strong lower semicontinuity coincide.

To invoke the fact that according to the Eberlein–Šmuljan theorem every bounded sequence in a reflexive Banach space has a weakly convergent subsequence, we need to assume that the functional F grows outside of bounded sets.

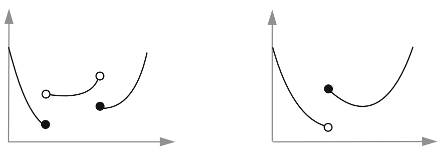

Fig. 2.12 A function that is lower semicontinuous (*left*) and a function that is not lower semicontinuous (*right*)

Definition 2.2 The functional $F : X \to \mathbb{R} \cup \{+\infty\}$ is called *(weakly) coercive* if for every sequence $(v_n)_{n\in\mathbb{N}} \subset X$ with $\|v_n\| \to \infty$, we have $F(v_n) \to \infty$ as $n \to \infty$.

The following theorem can be generalized in several directions. It is formulated in a way that is applicable to many of the variational problems discussed above.

Theorem 2.1 (Direct method in the calculus of variations) *Assume that $F : X \to \mathbb{R} \cup \{+\infty\}$ is weakly lower semicontinuous, coercive, bounded from below, and there exists $v_0 \in X$ with $F(v_0) \in \mathbb{R}$. Then F has a minimizer.*

Proof The proof follows in three steps.
Step 1: Since F is bounded from below, there exists an infimizing sequence $(v_n)_{n\in\mathbb{N}} \subset X$ with $\lim_{n\to\infty} F(v_n) = \inf_{v'\in X} F(v')$.
Step 2: The assumed coercivity of F implies that the sequence $(v_n)_{n\in\mathbb{N}}$ is bounded and therefore, using that X is reflexive, we may extract a weakly convergent subsequence $(v_{n_k})_{k\in\mathbb{N}}$ with weak limit $v \in X$.
Step 3: Due to the weak lower semicontinuity, we have $F(v) \le \liminf_{k\to\infty} F(v_{n_k})$ and therefore it follows that

$$F(v) \le \liminf_{k\to\infty} F(v_{n_k}) = \lim_{k\to\infty} F(v_{n_k}), = \inf_{v'\in X} F(v'),$$

i.e., since $F(v) \ge \inf_{v'\in X} F(v')$ we have $F(v) = \inf_{v'\in X} F(v')$ which proves the theorem. □

Remark 2.2 If a variational problem is formulated on a subset $A \subset X$, then we need to impose that A be weakly closed to ensure that the weak accumulation points of a bounded sequence belong to A. This is equivalent to the condition that the *indicator functional* $I_A : X \to \mathbb{R} \cup \{+\infty\}$, defined by $I_A(v) = 0$ for $v \in A$ and $I_A(v) = +\infty$ otherwise, be weakly lower semicontinuous. By Mazur's lemma, it suffices that A be convex and closed.

Examples 2.1 (i) The Dirichlet energy $I(u) = (1/2)\int_\Omega |\nabla u|^2 \,\mathrm{d}x$ is weakly lower semicontinuous since according to a binomial formula, we have

$$\int_\Omega |\nabla u|^2 \,\mathrm{d}x - \int_\Omega |\nabla u_n|^2 + \int_\Omega |\nabla(u-u_n)|^2 \,\mathrm{d}x = 2\int_\Omega \nabla u \cdot \nabla(u-u_n)\,\mathrm{d}x,$$

and if $u_n \rightharpoonup u$ in $H^1(\Omega)$, i.e., $\int_\Omega \nabla u \cdot \nabla(u-u_n)\,\mathrm{d}x \to 0$, this implies that $I(u) \le \liminf_{n\to\infty} I(u_n)$. The coercivity of I follows from a Poincaré inequality.
(ii) Simple examples such as Weierstraß' example show that not every minimization problem has a solution. By constructing an infimizing sequence consisting of Lipschitz continuous functions, one can verify that the functional

$$I(y) = \int_{(-1,1)} (xy'(x))^2 \,\mathrm{d}x$$